

# A study of non-parallel and nonlinear effects on the localized receptivity of boundary layers

By J. D. CROUCH AND P. R. SPALART

Boeing Commercial Airplane Group, PO Box 3707, M/S 7H-90, Seattle WA 98124-2207, USA

(Received 19 November 1993 and in revised form 7 November 1994)

The acoustic receptivity due to localized surface suction in a two-dimensional boundary layer is studied using a finite-Reynolds-number theory and direct numerical simulation of the Navier–Stokes equations. Detailed comparisons between the two methods are used to determine the bounds for application of the theory. Results show a 4% difference between the methods for receptivity in the neighbourhood of branch I with low suction levels, low acoustic levels, and a moderate frequency; we attribute this difference to non-parallel effects, not included in the theory. The difference is larger for receptivity upstream of branch I, and smaller for receptivity downstream of branch I. As the peak suction level is increased to 1% of the free-stream velocity, the simulations show a nonlinear deviation from the theory. Suction levels as small as 0.1% are shown to have a significant effect on the instability growth between branch I and branch II. Increasing the acoustic amplitude to 1% of the steady free-stream velocity produces no significant nonlinear effect.

---

## 1. Introduction

The transition to turbulence in boundary layers can be linked to the nonlinear development of unsteady velocity fluctuations. These velocity disturbances can result from free-stream perturbations, from surface variations (in geometry or transpiration velocity), or from a combination of the two. The character of the transition process depends on the structure and magnitude of the initial disturbance field; for example, small initial amplitudes may lead to the excitation of linear instability modes, whereas large initial amplitudes can directly trigger transition, bypassing the linear instabilities. For small to moderate disturbance amplitudes, the growth of the disturbance is described by stability theory. However, the stability analysis does not account for the initial excitation of the disturbance modes. The initial conditions for the stability analysis are derived from receptivity theory. When the disturbance modes are travelling waves (e.g. Tollmien–Schlichting (TS) waves or unsteady cross-flow vortices), the receptivity often involves the interaction of free-stream disturbances with steady disturbances resulting from the surface variation. The disturbance interactions can lead to both localized and non-localized excitation of the boundary-layer instabilities. Here, we focus on localized receptivity.

The earliest theoretical studies of localized receptivity are based on asymptotic methods (Goldstein 1985; Ruban 1985). These studies demonstrate the mechanism by which an acoustic disturbance can excite an instability wave through localized scattering. A local variation in surface geometry produces a steady velocity perturbation within the boundary layer. This steady disturbance is characterized by a broad spectrum of Fourier modes. The acoustic wave modulates this steady field to produce a spectrum of travelling waves. Downstream of the surface variation, the travelling-wave field is dominated by the most unstable eigenmode. A local variation

in surface transpiration can also provide the scattering necessary for receptivity (Heinrich, Choudhari & Kerschen 1988). The reviews of Goldstein & Hultgren (1989) and Kerschen (1989) provide additional discussion about the different localized-receptivity mechanisms which have been considered.

In the asymptotic analysis, the surface variation is taken to be upstream of or near the lower branch of neutral stability (branch I), and the scaling of the Reynolds number and frequency is coupled by the variation along the neutral curve. An expansion in inverse powers of the Reynolds number then leads to the nonlinear triple-deck equations governing the disturbance (Goldstein 1985). For small amplitudes of the surface perturbation, the triple-deck equations can be linearized – thus permitting a closed-form solution for the receptivity amplitude. This linearization is equivalent to applying the locally parallel basic-flow assumption. When the surface perturbation is ‘large’, the triple-deck equations can be solved numerically (Bodonyi *et al.* 1989; Bodonyi & Duck 1992). This provides a solution which is nonlinear (in terms of the surface-perturbation amplitude) and non-parallel (within the context of the triple-deck equations). However, the solution is linear in terms of the free-stream-disturbance amplitude and is also based on the large-Reynolds-number limit with the requirement that the boundary layer does not undergo massive separation.

Localized receptivity has also been studied using formulations based on the Orr–Sommerfeld equation (Zhigulev & Fedorov 1987; Crouch 1992; Choudhari & Streett 1992; Hill 1993). These formulations provide results which are based on finite Reynolds numbers and are valid both near and away from the lower branch of neutral stability (branch I). These approaches do not link the frequency and Reynolds number through their relative scaling, thus enabling a study of frequency effects at finite Reynolds numbers. The basic flow is assumed to be locally parallel and both the free-stream and surface-variation amplitudes are assumed to be small. The surface variation produces a locally ‘non-parallel’ contribution to the mean flow. The finite-Reynolds-number results for surface roughness are in very good agreement with experiments of Saric, Hoos & Radeztsky (1991) and simulations of Spalart (1993). At large Reynolds numbers (low frequencies), the results approach the values calculated from the linear asymptotic theory (Crouch 1992).

In this study, we consider localized acoustic receptivity due to surface suction using the finite-Reynolds-number theory and direct numerical simulations of the Navier–Stokes equations. The results are directly relevant to laminar-flow-control applications and indirectly relevant to other surface variations such as roughness. The effects of non-parallelism and nonlinearity are investigated by comparing results from the two methods. This study provides guidelines on the range of validity of the theory. It also provides a check on the algebra and programming errors for both methods.

## 2. Formulation

The flow is governed by the two-dimensional incompressible Navier–Stokes equations. We consider a flat-plate boundary layer with velocities  $(u, v)$  corresponding to the streamwise  $x$  and surface-normal  $y$  directions, respectively. All quantities are non-dimensionalized using the free-stream velocity  $U_\infty$  and the reference length  $\delta_r = (\nu x^*/U_\infty)^{1/2}$ . This introduces the Reynolds number  $R = U_\infty \delta_r / \nu$ .

The surface transpiration is represented by the boundary condition

$$u = 0, \quad v = \pm \epsilon_s H(x) \quad \text{at} \quad y = 0, \quad (1)$$

$$H(x) = e^{-(x-x_0)^2/\sigma^2}, \quad (2)$$

where  $x_0$  is the streamwise location of the centre of the Gaussian distribution and  $v(x, y = 0) < 0$  for suction. In the incompressible limit, an acoustic free-stream disturbance leads to the boundary condition

$$u \rightarrow 1 + \epsilon_a e^{-i\omega t} \quad \text{as } y \rightarrow \infty. \quad (3)$$

The small parameters  $\epsilon_s$  and  $\epsilon_a$  correspond to the transpiration level and the acoustic amplitude, respectively.

### 2.1. Perturbation theory

In the perturbation theory, we consider  $\epsilon_a, \epsilon_s \ll 1$  and expand the velocity in the form

$$v(x, y, t) = v_0(y) + \epsilon_a v_a(y, t) + \epsilon_s v_s(x, y) + \epsilon_a \epsilon_s v_{as}(x, y, t) + O(\epsilon_a^2) + O(\epsilon_s^2). \quad (4)$$

The first term in the expansion is the Blasius profile under the assumption of quasi-parallel flow. The quasi-parallel-flow approximation locally neglects the weak  $x$ -variation of the boundary layer leading to the non-homogeneous Orr–Sommerfeld equation for each of the disturbance velocities. At  $O(\epsilon_a)$ , the unsteady flow is decoupled from the surface transpiration. This component of velocity represents the Stokes flow induced by the acoustic wave of frequency  $\omega$ . The surface transpiration produces a steady disturbance field at  $O(\epsilon_s)$ . The interaction of the steady and unsteady disturbances at  $O(\epsilon_a \epsilon_s)$  then produces an unsteady disturbance with length and time scales that may match those of the natural boundary-layer instabilities. Although the  $O(\epsilon_a \epsilon_s)$  solution is generated through a nonlinear interaction, this component is linear with respect to both  $\epsilon_a$  and  $\epsilon_s$ . The  $O(\epsilon_a^2)$  and  $O(\epsilon_s^2)$  disturbances are not included since they do not contribute to the receptivity at this order; this can be verified by harmonic balance.

The surface transpiration velocity  $H(x)$ , the steady field  $v_s(x, y)$ , and the resulting unsteady field  $v_{as}(x, y, t)$  are represented by Fourier transforms in the streamwise direction. In evaluating the inverse Fourier transform, the TS component of  $v_{as}$  is given by the residue associated with a pole singularity at  $\alpha = \alpha_{TS}$  (where  $\alpha_{TS}$  is the streamwise wavenumber for the least-stable eigenmode). The disturbance amplitude, defined as the maximum of the  $u_{as}$ -velocity component, is given by

$$A_0 = |\epsilon_a \epsilon_s K \tilde{H}(\alpha_{TS})|. \quad (5)$$

The function  $K$  is the response residue for the conditions  $(\omega, \alpha_{TS}, R_0)$  and  $\tilde{H}(\alpha_{TS})$  is the Fourier transform of  $H(x)$  evaluated at the eigenmode wavenumber. Additional details about the perturbation theory are given by Crouch (1992) in the context of localized-roughness receptivity. Choudhari & Streett (1992) provide a similar presentation of the theory, including results for localized suction. The receptivity amplitude  $A_0$  provides the disturbance level at the receptivity source  $x_0$ , or  $R_0$ . To enable a comparison of the relative strength of the receptivity occurring at different streamwise locations, we also define an effective branch-I amplitude  $A_I$  given by

$$A_I = A_0 \exp\left(-\int_{R_0}^{R_I} 2\alpha_{TSi}(R) dR\right), \quad (6)$$

where  $R_I$  is the branch-I Reynolds number. This is the branch-I disturbance amplitude which would produce a response equivalent to  $A_0$  downstream.

### 2.2. Numerical simulation approach

The numerical approach was used earlier by Spalart (1993), but few details were given. Using a closely related method Bertolotti, Herbert & Spalart (1992) presented results for the evolution of TS waves in Blasius flow, demonstrating full non-parallel and

nonlinear capabilities. The simulations are ‘spatial’ even though a Fourier method is used in  $x$  (Spalart, Moser & Rogers 1991); this is a result of applying a ‘fringe method’. The very close agreement between the PSE and the DNS reported in that paper led to a high degree of confidence in both approaches. The variant of the fringe method used here is different from that of Bertolotti *et al.*, primarily because a laminar velocity field ( $U_B$  in their notation) is not available due to the suction and the acoustic forcing. The variant used here is very close to that described by Spalart & Watmuff (1993, hereafter referred to as SW), although they treated turbulent flow. As their discussion was extensive, here we only discuss differences with that work.

The first extension is that the  $U_0$  velocity field now includes suction at the wall, as well as the acoustic fluctuation in the free stream (i.e. the non-homogeneous boundary conditions). This field is also time-dependent, which introduces the term  $-\partial U_0/\partial t$  in the right-hand side of the momentum equation, SW equation (9). The sum of a decaying exponential in  $y$  and the Stokes-wave solution is a convenient choice to introduce the free-stream boundary condition (3). For the suction boundary condition (1), (2) it is more convenient to work in Fourier space in  $x$ . Divergence-free velocity fields that are non-zero at the wall and decay in the free stream are constructed from the Laplace solution  $\exp(-ky)$ , where  $k$  is the wavenumber, and other exponential factors much like in SW equation (7). These are adjusted to be infinitesimal outside the expected boundary layer, so as not to introduce vorticity there. A simplification, compared with SW, is that no pressure gradient is applied. As a result, only the  $k = 0$  form of SW equation (7) is needed, and the  $U_3$  correction (SW, §3.3) is unnecessary. The  $S'$  term of SW equation (9) is also absent.

The other difference, relative to SW, is in the use of the  $U_2$  term. In SW the  $S$  parameter in the fringe term  $U_2$  was adjusted to effect a moderate reduction in the boundary-layer thickness, by a factor of about 2, without suppressing the turbulence; note that a mature turbulent inflow state was desired. Here, in contrast, it takes larger values and is adjusted to produce a thickness reduction by a factor of about 10 – with two results. The first is that the boundary layer, being very thin at the inflow, rapidly evolves into a Blasius profile. This is confirmed by the shape factor, which reaches 2.58 upstream of the suction slot, and the product  $C_f R_\theta$ , which reaches 0.441. The virtual origin of that Blasius flow can then be accurately determined so as to correctly locate the suction slot. If we add this adjustment region to the fringe region proper (in which extra terms are active, see SW) we find that the useful region represents about 80% of the period in  $x$ . The second result of the larger  $S$  values is that the TS waves are suppressed in the fringe region, both by the low thickness Reynolds number ( $R_{\theta^*} < 300$ ) and by the compression imposed by  $U_2$ . The suppression is not complete, but the residual amplitude can be made small enough compared with the receptivity amplitude – if needed by widening the fringe.

Grid-refinement results are discussed by Spalart (1993). We use the same resolution in  $y$ . For the  $x$ -direction, we verify that the  $H$ -function in (2) is resolved with very little ringing; we also find that the spurious amplitude upstream of the suction slot is about two orders of magnitude lower than the receptivity amplitude. This spurious amplitude reflects perturbations not fully suppressed by the fringe terms, as well as truncation errors propagated by the spectral method. All the amplitudes quoted are the peak r.m.s. value of the streamwise velocity fluctuation, versus  $y$ , at a given  $x$ -location.

The calculation of a receptivity amplitude requires a ‘reference simulation’ which includes acoustic forcing, but no suction. By subtracting the reference solution from the full solution and extracting the time-dependent content of that difference we isolate the interaction component,  $O(\epsilon_a \epsilon_s)$ , from the steady suction component,  $O(\epsilon_s)$ , and the

acoustic component,  $O(\epsilon_a)$ . The acoustic component depends on the inflow conditions, and in any case is not identical to the Stokes wave, because we are using moderate frequencies and Reynolds numbers. Thus it is essential to isolate it, especially for small values of  $\epsilon_s$ .

The receptivity amplitude is determined by measuring the  $O(\epsilon_a \epsilon_s)$  disturbance magnitude at some downstream reference location  $R_{II}$  (branch II for the linear stability problem). The amplitudes  $A_0$  and  $A_I$  are then calculated from the downstream amplitude using

$$A_0 = A(R_{II}) e^{-N_s(R_0)} \quad (7)$$

$$A_I = A(R_{II}) e^{-N_s(R_I)}, \quad (8)$$

where  $A(R_{II})$  is the amplitude at  $R_{II}$  and  $N_s(R)$  is the  $N$ -factor between  $R$  and  $R_{II}$  based on the maximum of the  $u$ -profile. The function  $N_s(R) = \ln[A(R_{II})/A(R)]$  is calculated from a separate numerical simulation of a small-amplitude wave introduced upstream of  $R$  in the presence of suction. This function is the non-parallel equivalent of the integrated growth rate from quasi-parallel theory (including the suction effects on the instability growth). For the frequency and suction locations considered, the excited disturbance is very close to a pure TS wave when it reaches branch II. As a result, the choice of the downstream reference location has very little influence on the calculated receptivity amplitudes.

### 3. Results

In the presentation of results we focus on the receptivity amplitude since this is the most important information provided by the theory. The receptivity amplitude can be used in conjunction with stability theory to make estimates on the transition location for flows of practical interest. The results are all for the frequency  $F = 10^6 \omega/R = 56$ . The value of  $\sigma$  is chosen to maximize  $\tilde{H}(\alpha_{TS})$  at  $R_I \approx 575$ ; this gives  $\sigma = 14.2$ , in terms of the local branch-I scaling. The dimensional value of  $\sigma$ ,  $8160\nu/U_\infty$ , is held constant for all cases considered.

We first consider the influence of the suction location  $R_0$  on the receptivity amplitude. Figure 1 shows the variation of the receptivity amplitude at the suction location  $A_0$  as a function of  $R_0$ . The suction level and the acoustic amplitude for the simulation results are  $\epsilon_s = 10^{-5}$  and  $\epsilon_a = 10^{-4}$ , respectively. These values ensure that the results are linear. The receptivity level shows a strong increase as the suction is moved upstream. The theory is in good agreement with the simulation results for Reynolds numbers  $R \geq R_I$ . At branch I, the difference between the two methods is approximately 4%. The lower prediction of the theory becomes more significant upstream of branch I. The difference between the results at  $R = 400$  is 6.5–11.2%. There is an uncertainty associated with the simulation value  $N_s$  at  $R = 400$  due to local transients (Bertolotti *et al.* 1992); the two points shown in figure 1 provide a band around the actual value. The principal differences between the theory and simulation can be attributed to non-parallel effects, not accounted for in the theory. The perturbation expansion provides a consistent approximation for small levels of  $\epsilon_s$  and  $\epsilon_a$ . However, the growth of the boundary layer is neglected. The comparison between the simulation and theory shows that neglecting the weak boundary-layer growth is an acceptable approximation. Significant deviations are limited to the region upstream of branch I.

In order to better illustrate the impact these disturbances can have on transition, we recast the receptivity amplitudes in terms of effective branch-I amplitudes. Figure 2

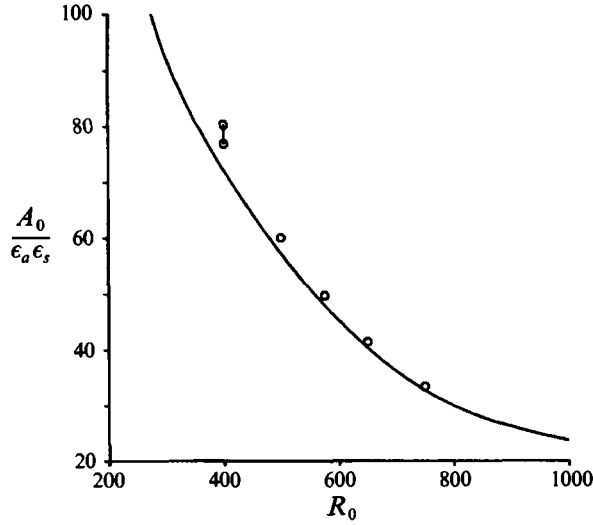


FIGURE 1. Receptivity amplitude at the suction location,  $A_0/\epsilon_a\epsilon_s$ , as a function of  $R_0$ . Solid line – perturbation theory, symbols – numerical simulation.

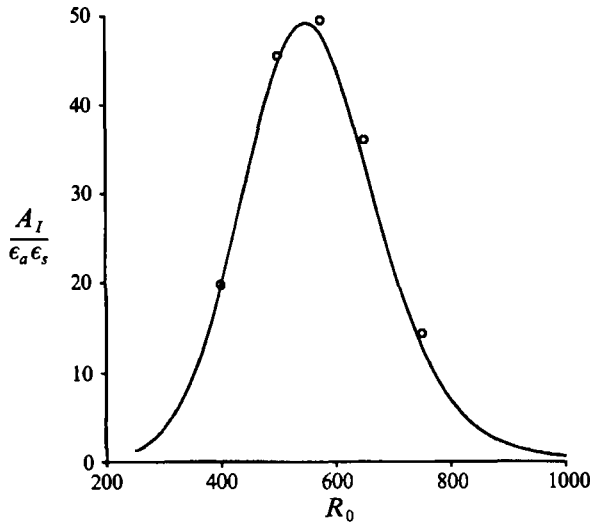


FIGURE 2. Effective receptivity amplitude at branch I,  $A_I/\epsilon_a\epsilon_s$ , as a function of  $R_0$ . Solid line – perturbation theory, symbols – numerical simulation.

shows the variation of  $A_I$  with  $R_0$ . Now that the disturbance growth is accounted for, the strongest receptivity occurs for suction locations near branch I. The maximum level of  $A_I$  is just upstream of  $R_I$ ; this has also been shown for receptivity to cross-flow vortices (Crouch 1993; Herbert & Lin 1993). The agreement between the theory and the simulation is unchanged for  $R \approx R_I$ . Upstream of branch I, the agreement is substantially better. This results from a cancellation between the non-parallel effects on the receptivity and the non-parallel effects on the linear growth. The degree of cancellation may not be the same for other frequencies. The quasi-parallel approximation provides accurate results for the linear receptivity amplitudes near branch I (the region of highest potential impact for transition).

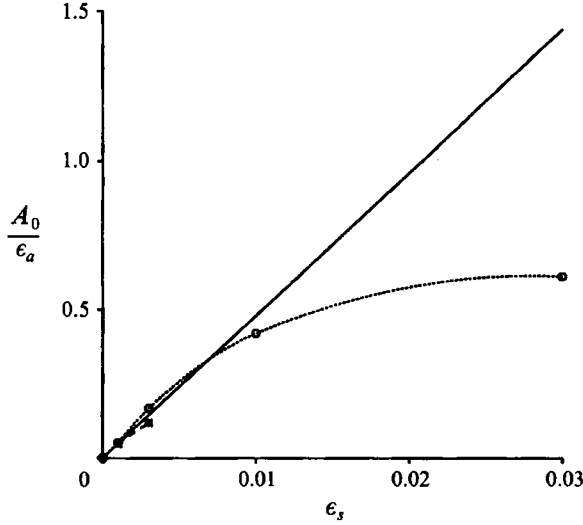


FIGURE 3. Variation of the receptivity amplitude  $A_0/\epsilon_a$  with the magnitude of the transpiration velocity  $\epsilon_s$  for the condition  $R_0 = 575 \approx R_I$ . Solid line – perturbation theory, symbols – numerical simulation  $A(R_I) e^{-N_s(R_0)}$  for suction ( $\circ$ ) and blowing ( $*$ ).

We now consider the effects of increasing the magnitude of the surface transpiration velocity. Figure 3 shows the variation of  $A_0$  with  $\epsilon_s$ , for both suction  $v(x, y = 0) < 0$  and blowing  $v(x, y = 0) > 0$ . The suction strip is located near branch I,  $R_0 \approx R_I$ , where the receptivity has the greatest impact (i.e.  $A_I \approx A_0$ ). The maximum suction level considered is  $\epsilon_s = 0.03$ ; in the asymptotic scaling of Heinrich *et al.* (1988) and Bodonyi & Duck (1992), the value of  $\epsilon_s = 0.03$  corresponds to a suction velocity of  $V_s^* = -R^{3/4} \epsilon_s \approx -3.5$ . For small transpiration velocities,  $\epsilon_s \leq 0.1\%$ , the simulation results are approximately the same for suction and blowing. The theory is in good agreement with the simulations for this range of  $\epsilon_s$ . There is no distinction between suction and blowing in the perturbation results at  $O(\epsilon_a \epsilon_s)$ . The simulation results show a near-linear dependence on  $\epsilon_s$  for values up to 1%. Larger values of  $\epsilon_s$  result in significant nonlinear effects on the receptivity. In terms of the asymptotic scaling,  $\epsilon_s = 1\%$  corresponds to an order-one suction velocity (Heinrich *et al.* 1988). Thus the asymptotic theory would predict significant nonlinear effects at this suction level. The virtual origin of the Blasius flow that is re-established downstream of the slot is shifted by about 50 units in  $R$  for  $\epsilon_s = 1\%$ . This amount of suction is well beyond the levels used for typical laminar-flow-control applications. However, similar nonlinear effects will occur for large-amplitude surface bumps which are encountered in practical applications (Saric *et al.* 1991; Bodonyi *et al.* 1989). The difference between the suction and blowing results at  $\epsilon_s = 0.3\%$  would be removed if the source location,  $R_0$ , used in (7) was shifted toward the downstream edge of the suction slot. This suggests that the effective origin for the receptivity is just downstream of the centre of the suction distribution. The large-suction nonlinear effect on the receptivity decreases the initial amplitude well below the linear value. The difference between the theory and the nonlinear simulation at  $\epsilon_s = 3\%$  is approximately 57% of the theoretical value.

Potential nonlinear effects due to large acoustic amplitudes have also been investigated. Numerical simulations were conducted with  $\epsilon_a = 10^{-3}$  and  $10^{-2}$  at the conditions  $\epsilon_s = 10^{-3}$ ,  $R_0 = 575$ . For the experimental conditions of Saric *et al.* (1991), these amplitudes would correspond to sound levels of 104 and 124 dB, respectively.

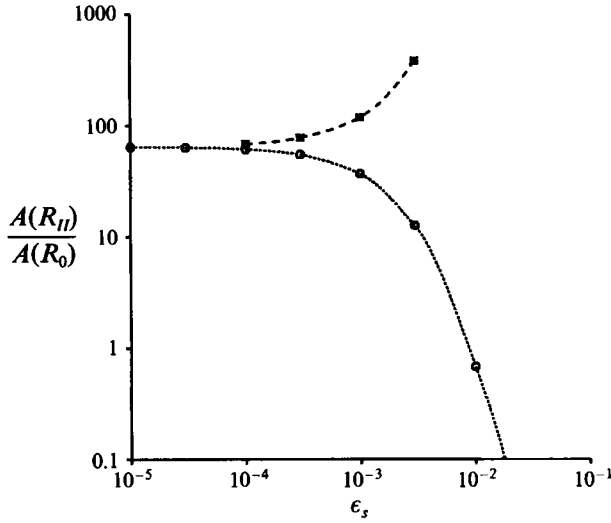


FIGURE 4. Variation of the amplitude-growth ratio  $A(R_{II})/A(R_0)$  with the magnitude of the transpiration velocity  $\epsilon_s$  for the condition  $R_0 = 575 \approx R_I$ . Results for suction ( $\circ$ ) and blowing ( $\star$ ).

These larger values of  $\epsilon_a$  had no effect on the receptivity amplitudes. The relative insensitivity to the magnitude of  $\epsilon_a$  can be explained by a simple order-of-magnitude analysis. Since the sound field is given by a discrete frequency, the first modification (due to large  $\epsilon_a$ ) of the  $O(\epsilon_a \epsilon_s)$  receptivity occurs at  $O(\epsilon_a^3 \epsilon_s)$ . Thus for an amplitude of  $\epsilon_a = 10^{-2}$ , the next term in the expansion is  $O(10^{-4})$  smaller. Even if the coefficient of the  $O(\epsilon_a^3 \epsilon_s)$  term were large, its contribution is likely to be small if  $\epsilon_a \leq 1\%$ .

Finally, we consider the total effects of the suction, or blowing, on the amplitude measured downstream,  $A(R_{II})$ . The downstream amplitude is typically used to infer the receptivity amplitude in experiments – see, for example, Saric *et al.* (1991). The value of  $A(R_{II})$  includes the combined effects of receptivity and modifications to the linear growth. Figure 4 shows the variation of the growth ratio  $A(R_{II})/A(R_0)$  as a function of  $\epsilon_s$  for suction and blowing. For  $\epsilon_s < 0.1\%$ , the local surface transpiration has a negligible effect on the instability growth. The growth is significantly modified for  $\epsilon_s \geq 0.1\%$ . The total disturbance, measured downstream, is the product of the receptivity amplitude  $A_0$  and the growth ratio  $A(R_{II})/A(R_0)$ . Therefore, the total amplitude  $A(R_{II})/\epsilon_a$  varies linearly with  $\epsilon_s$  for  $\epsilon_s < 0.1\%$ . For  $\epsilon_s \geq 0.1\%$ ,  $A(R_{II})/\epsilon_a$  shows a nonlinear variation due to modifications to the instability growth. The effect of nonlinearity in the receptivity does not affect  $A(R_{II})$  until  $\epsilon_s$  reaches a level of  $1\%$ . A similar behaviour can be expected for large surface bumps. As the bump height is increased, the initial effect will be to enhance the disturbance growth; this will be followed by a modification of the receptivity amplitude if the bump height becomes sufficiently large.

#### 4. Conclusions

This study shows good agreement between the Orr–Sommerfeld-based receptivity theory and numerical simulations at a moderate frequency of  $F = 56$  in Blasius flow. Non-parallel effects, which are neglected in the theory, change the receptivity amplitude by less than  $4\%$  for receptivity in the neighbourhood of branch I. Upstream of branch I, the effects become more significant; however, these disturbances have less

potential for impacting transition. Nonlinear effects due to large suction levels lead to decreased receptivity for  $\epsilon_s > 1\%$ . Significant modifications to the linear growth occur at  $\epsilon_s \approx 0.1\%$  – below the value of  $\epsilon_s$  for nonlinear receptivity. These modifications produce a nonlinear variation in the total amplitude measured downstream. Large acoustic amplitudes  $\epsilon_a$ , for a single-frequency disturbance, have a negligible effect on the receptivity level. The receptivity theory provides an accurate basis for developing an amplitude-based method for transition prediction.

Mainframe computer time provided by NAS.

#### REFERENCES

- BERTOLOTTI, F. P., HERBERT, TH. & SPALART, P. R. 1992 Linear and nonlinear stability of the Blasius boundary layer. *J. Fluid Mech.* **242**, 441.
- BODONYI, R. J. & DUCK, P. W. 1992 Boundary-layer receptivity due to a wall suction control of Tollmien–Schlichting waves. *Phys. Fluids A* **4**, 1206.
- BODONYI, R. J., WELCH, W. J. C., DUCK, P. W. & TADJIFAR, M. 1989 A numerical study of the interaction between unsteady free-stream disturbances and localized variations in surface geometry. *J. Fluid Mech.* **209**, 285.
- CHOUHDARI, M. & STREETT, C. L. 1992 A finite Reynolds number approach for the prediction of boundary layer receptivity in localized regions. *Phys. Fluids A* **4**, 2495.
- CROUCH, J. D. 1992 Localized receptivity of boundary layers. *Phys. Fluids A* **4**, 1408.
- CROUCH, J. D. 1993 Receptivity of three-dimensional boundary layers. *AIAA Paper* 93-0074.
- GOLDSTEIN, M. E. 1985 Scattering of acoustic waves into Tollmien–Schlichting waves by small streamwise variations in surface geometry. *J. Fluid Mech.* **154**, 509.
- GOLDSTEIN, M. E. & HULTGREN, L. S. 1989 Boundary-layer receptivity to long-wave free-stream disturbances. *Ann. Rev. Fluid Mech.* **21**, 137.
- HEINRICH, R. A., CHOUHDARI, M. & KERSCHEN, E. J. 1988 A comparison of boundary layer receptivity mechanisms. *AIAA Paper* 88-3758.
- HERBERT, TH. & LIN, N. 1993 Studies of boundary-layer receptivity with parabolized stability equations. *AIAA Paper* 93-3053.
- HILL, D. C. 1993 Adjoint systems and their role in the receptivity problem for boundary layers. *CTR Manuscript* 146. Stanford.
- KERSCHEN, E. J. 1989 Boundary layer receptivity. *AIAA Paper* 89-1109.
- RUBAN, A. I. 1985 On the generation of Tollmien–Schlichting waves by sound. *Fluid Dyn.* **19**, 709.
- SARIC, W. S., HOOS, J. A. & RADEZTSKY, R. H. 1991 Boundary-layer receptivity of sound with roughness. In *Boundary Layer Stability and Transition to Turbulence*. FED-Vol. 114, pp. 17–22. ASME.
- SPALART, P. R. 1993 Numerical study of transition induced by suction devices. In *Near-Wall Turbulent Flows*, pp. 849–858. Elsevier.
- SPALART, P. R., MOSER, R. D. & ROGERS, M. M. 1991 Spectral methods for the Navier–Stokes equations with one infinite and two periodic directions. *J. Comput. Phys.* **96**, 297.
- SPALART, P. R. & WATMUFF, J. H. 1993 Experimental and numerical study of a turbulent boundary layer with pressure gradients. *J. Fluid Mech.* **249**, 337 (referred to herein as SW).
- ZHIGULEV, V. N. & FEDOROV, A. V. 1987 Boundary-layer receptivity to acoustic disturbances. *J. Appl. Mech. Tech. Phys.* **28**, 28.